Twenty-Seventh Symposium (International) on Combustion/The Combustion Institute, 1998/pp. 1057–1064

UNSTEADY FLAMELET MODELING OF TURBULENT HYDROGEN-AIR DIFFUSION FLAMES

H. PITSCH, M. CHEN AND N. PETERS
Institut für Technische Mechanik
RWTH Aachen
Templergraben 64
D-52056 Aachen, Germany

The unsteady flamelet model is applied in numerical simulations of a steady, turbulent, nitrogen-diluted hydrogen-air diffusion flame. An unsteady flamelet is solved interactively with a CFD solver for the turbulent flow and the mixture fraction field. Transient effects occurring in steady jet diffusion flames are discussed in terms of the relevant timescales. It is shown that radiation can be neglected and that the flame structure is hardly influenced by transient effects for the present case. However, for predictions of slow processes, like the formation of NO, unsteady effects have to be considered. The results predicted by the model are in reasonable agreement to experimental data for temperature, major species mass fractions, OH, and NO mole fractions. On the contrary, the use of steady flamelet libraries yields good results for flame structure and even OH concentrations, but NO is overpredicted by an order of magnitude. However, reasonably well-predicted NO concentrations can also be obtained by solving an unsteady flamelet as a postprocessing mode.

Introduction

Modeling of combustion in turbulent diffusion flames has been shown to be already rather successful [1]. The two combustion models that are mainly applied are the probability density function (PDF) transport equation approach [2,3] and the flamelet approach. The latter will be used and discussed in detail in the present study.

The common idea behind flamelet models is the separation of the numerical solution of the turbulent flow and mixture fields from the solution of the chemistry.

Applying the flamelet approach, transport equations for the moments of a conserved variable are solved. The conserved variable is chosen such that it describes the local mixture and is therefore called the mixture fraction. Turbulent mean values of the mass fractions of chemical components can then be calculated by using a presumed PDF of the mixture fraction, whose shape is determined by its statistical moments. Besides the PDF, the only requirement of the model is that there exists locally a unique relation between the mixture fraction and all scalar quantities like the species mass fractions and the enthalpy.

A universal coordinate transformation of the governing equations using the mixture fraction as independent coordinate yields the required relationship between the species concentrations and the mixture fraction in terms of the so-called flamelet equations [4,5], which are under some simplifying assumptions of the following kind:

$$\rho \frac{\partial T}{\partial t} - \rho \frac{\chi}{2}\left(\frac{\partial^2 T}{\partial Z^2} + \frac{1}{c_p}\frac{\partial c_p}{\partial Z}\frac{\partial T}{\partial Z}\right) + \frac{1}{c_p}\left(\sum_{k=1}^{N} h_k \dot{m}_k + \dot{q}_R''' - \mathcal{H}\right) = 0 \quad (1)$$

where t denotes the time, Z the mixture fraction, T the temperature, χ the scalar dissipation rate, ρ the density, c_p the specific heat capacity at constant pressure, and $\dot{q}_R'''$ the rate of radiative heat loss per unit volume. N and h_k are the number of chemical species and the enthalpy of species k, respectively. $\mathcal{H}$ accounts for the enthalpy flux by mass diffusion. The exact form for this term depends on the particular diffusion model and is given in Ref. [6] for the present work.

The flamelet model provides the advantage to include both finite-rate chemistry and the influence of the local mixture fraction gradients imposed by the flow field. These are expressed by the scalar dissipation rate, which appears as a parameter in the flamelet equations and must be modeled.

Although laminar flamelet models in non-premixed combustion have been successfully applied for predictions of mean values for temperature and species concentrations [7,8] and formation of pollutants such as NO_x [9] and soot [10], some aspects of laminar flamelet modeling in turbulent combustion are still unclear, as, for instance, the modeling of transient effects.

The purpose of this paper, is to discuss and to model transient effects in turbulent diffusion flames.

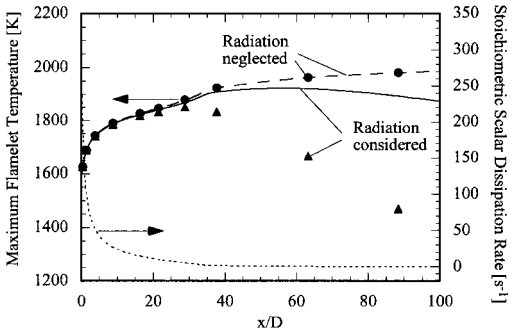

FIG. 1. Maximum temperature of an unsteady flamelet (*lines*) compared to steady flamelet solutions (*symbols*).

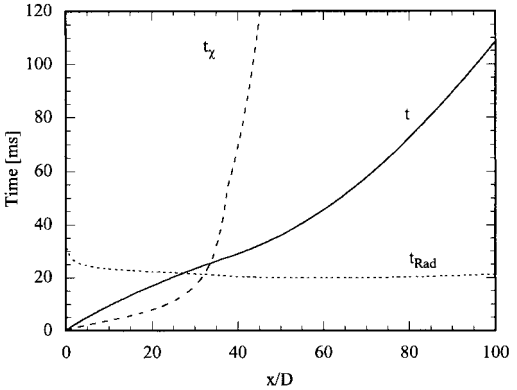

FIG. 2. Characteristic timescales.

The modeling will be done in the frame of a turbulent nitrogen-diluted hydrogen-air diffusion flame, which has previously been chosen as a standard test case for modeling of non-premixed combustion and is called H3-flame [11–14]. The results of the model will be compared to experimental data for temperature, major species, OH, and NO concentrations. In contrast to the work of Sanders et al. [9], NO concentrations are not calculated by the solution of transport equations for the turbulent mean values. Although it is known that the formation of NO involves slow reaction rates and can therefore not be predicted with a steady flamelet library concept, NO concentrations will be determined directly from the flamelet model by the use of unsteady flamelets.

Formulation

Transient Effects

The importance of transient effects in a steady turbulent jet diffusion flame has already been emphasized [4]. The deficiency of the steady-state flamelet approach is caused by the strong decay of the scalar dissipation rate along the jet axis on the one hand and by radiative heat losses on the other hand. The scalar dissipation rate χ, which can influence the flamelet solution significantly, decreases with x^{-4} along the axis, if x is the distance from the nozzle. Therefore, a flamelet that is transported downstream has to undergo strong changes. Several authors have shown experimentally [15] and in simulations of unsteady flamelets [16,17] that the chemical flamelet structure cannot follow rapid changes of the scalar dissipation rate instantaneously. To overcome the modeling problem, Haworth et al. [8] have proposed an ad hoc modification of the flamelet model, where an equivalent quasi-steady strain rate is used to account for transient effects. Ferreira [18] has shown that for the description of diffusion flame stabilization, transient effects have to be included and accounts for these by the use of libraries with unsteady flamelets.

To study the transient effects in the flame investigated in this paper, the maximum flamelet temperature of unsteady flamelets with and without radiation effects is compared with steady flamelets in Fig. 1. The unsteady flamelet has been calculated as a function of the flamelet time, which can be related to the distance from the nozzle as

$$t = \int_0^x \frac{1}{u(x')|(\tilde{Z} = Z_{st})}\, dx' \qquad (2)$$

where $\tilde{Z}$ is the favre average of the mixture fraction and $u(x)|(\tilde{Z} = Z_{st})$ is the axial velocity component at the radial position, where $\tilde{Z} = Z_{st}$. The temporal evolution of the scalar dissipation rate that has been used to perform the unsteady calculation is also depicted in Fig. 1. It is determined from the flow-field solution as domain average of the conditional scalar dissipation rate at stoichiometric mixture $\langle\widehat{\chi_{st}}\rangle$, which is defined in equation 15. The steady flamelets are each computed with the scalar dissipation rate at the respective distance from the nozzle.

Obviously, there is no remarkable difference in the maximum temperatures if radiation is not considered. The reason can be explained as follows: In the flamelet equations, the scalar dissipation rate appears as a diffusion coefficient in mixture fraction space. A characteristic diffusion time t_χ that is needed to transport mass and energy over a distance ΔZ in mixture fraction space may be defined as

$$t_\chi = \frac{\Delta Z^2}{\chi_{st}} \qquad (3)$$

Here, the distance ΔZ is estimated as $\Delta Z = Z_{st}$. The diffusion time t_χ is compared for $\Delta Z = Z_{st}$ to the flamelet lifetime t in Fig. 2, revealing that in the beginning the diffusion time is short due to the high scalar dissipation rate and the flamelet is able to follow changes in the scalar dissipation rate rapidly. After 30 ms, the characteristic diffusion time is longer

than the flamelet lifetime and increases rapidly in the following. At this time, however, the flamelet is already close to the equilibrium, and changes of the flamelet structure due to changes of the scalar dissipation rate are small.

The effect of radiation can be discussed similarly. In turbulent jet flames close to the nozzle due to steep gradients, the diffusive transport of heat is usually so high that the influence of radiation is negligible. Far downstream of the nozzle, however, due to decreased axial velocity, the residence times are long enough to allow radiative heat losses to be important. This can be shown by comparing the relevant timescales.

A commonly used approach to model the rate of radiative heat loss per unit volume $\dot{q}'''_R$ for hydrogen flames in the optically thin limit is given by [19]

$$\dot{q}'''_R = 2\sigma(T^4 - T_u^4)p_{H_2O}\alpha_{P,H_2O} \tag{4}$$

where σ is the Stefan–Boltzmann constant, T_u the background temperature, α_{P,H_2O} the Planck mean absorption coefficient of gaseous H_2O, and p_{H_2O} the partial pressure of H_2O. A characteristic radiation time in a diffusion flame, which is needed to decrease the maximum flame temperature by ΔT, may then be defined as

$$t_{Rad} = \frac{(\rho c_p)_{st}\Delta T}{\dot{q}'''(T_{max})} \tag{5}$$

where the index st denotes stoichiometric conditions. The characteristic radiation time for decreasing the maximum flamelet temperature by 50 K ($\Delta T = 50$ K) is compared to the flamelet lifetime in Fig. 2. After a short time, t_{Rad} remains almost constant at about $t_{Rad} \approx 20$ ms. This means that radiation is unimportant at least during the first 20 ms. Thereafter, radiation influences the flamelet, but still, the radiation time and the flamelet lifetime remain in the same order of magnitude, which indicates that radiative effects cannot occur instantaneously.

This is also shown in Fig. 1, where the maximum temperature from the calculation of an unsteady flamelet with radiation effects included is compared to the corresponding steady flamelets. Radiation cannot influence the solution within the first 20 ms due to the short residence and diffusion time. When $t_{Rad} < t \approx t_\chi$ at approximately $x/D = 30$, the temperature drop by radiation starts to become significant for the steady case. In the unsteady flamelet, the radiation effect appears shortly later, but because there is a relaxation effect due to the unsteady term, the temperature decrease in the unsteady flamelet is much slower.

From the discussion of the transient effects for the investigated flame, we conclude that radiation is important if both the characteristic diffusion and residence times are larger than the radiation time. Results predicted by the use of steady flamelet libraries considering radiation are therefore unrealistic. If steady-state flamelets should still be used, the neglect of radiative effects leads to better results for flow-field predictions, because the slight overprediction of the temperature is not expected to have a strong influence. For predictions of temperature-sensitive quantities like NO formation, however, both temperature changes by radiation and the transient effect on the NO-formation process have to be considered.

Model for the Conditional Scalar Dissipation Rate

The use of equation 1 requires the modeling of the scalar dissipation rate. Under the assumption that laminar flamelets in turbulent non-premixed combustion can be represented by an infinite one-dimensional mixing layer, the flame structure can also be described by counterflow diffusion flames [4]. Analytic expressions for the scalar dissipation rate in these configurations have been derived under simplifying assumptions [4,20] and can be described by

$$\chi(Z) = \chi_{st} f(Z) \tag{6}$$

where χ_{st} is the scalar dissipation rate at the stoichiometric mixture fraction Z_{st}.

Bish and Dahm [21] have shown that laminar flamelets in turbulent diffusion flames do not necessarily extend from pure air to pure fuel but that the instantaneous mixture fraction shows local extrema. They have therefore used the relation for the infinite mixing layer with partial premixed boundary conditions. However, in Ref. [22], a one-dimensional mixing layer with fuel originating from the axis of symmetry in an infinite oxidizer environment is regarded as a better representation for flamelets in turbulent diffusion flames, because this semi-infinite mixing layer reveals a local maximum of the fuel concentration and allows the description of complete mixing of the fuel with the surrounding air.

In this configuration, the governing equation for the mixture fraction can be written as

$$\rho\frac{\partial Z}{\partial t} - \frac{\partial}{\partial y}\left(\rho D_Z \frac{\partial Z}{\partial y}\right) = 0 \tag{7}$$

with the boundary conditions $Z(y \to \infty) = 0$ and $\partial Z/\partial y|_{y=0} = 0$, where D_Z is the diffusion coefficient of the mixture fraction and y the spatial coordinate. Introducing the similarity coordinate η as

$$\eta = \frac{1}{2\sqrt{(\rho^2 D_Z)_\infty t}}\int_0^y \rho dy' \tag{8}$$

a particular solution of equation 7 under the assumption $\rho^2 D_Z = (\rho^2 D_Z)_\infty$ is given by the Gaussian function in the form

$$Z = \frac{A}{2\sqrt{D_{Z\infty}t}}e^{-\eta^2} \tag{9}$$

where A is a constant. If the maximum-occurring value for the mixture fraction is denoted by Z_{max}, with the definition of the scalar dissipation rate $\chi = 2D_Z (\partial Z/\partial y)^2$, an analytic expression for the mixture fraction dependence of χ can be expressed as [22]

$$\chi = \chi_{st} \frac{Z^2}{Z_{st}^2} \frac{\ln Z/Z_{max}}{\ln Z_{st}/Z_{max}} \tag{10}$$

which also satisfies equation 6. This model will be used here for $Z_{max} = 1$.

With equation 6, χ depends on χ_{st} and Z, which are both fluctuating quantities. Assuming that these are statistically independent, the turbulent mean value of the scalar dissipation rate can be expressed by

$$\tilde{\chi} = \int_{\chi_{st}} \chi'_{st} \tilde{P}(\chi'_{st}) d\chi'_{st} \int_Z f(Z) \tilde{P}(Z) dZ \tag{11}$$

where the first integral defines the mean scalar dissipation rate conditioned on Z_{st} as

$$\langle \chi_{st} \rangle = \int_{\chi_{st}} \chi'_{st} \tilde{P}(\chi'_{st}) d\chi'_{st} \tag{12}$$

Hellström [23] suggested to equate the right-hand side of equation 11 with the commonly used model for the unconditional mean scalar dissipation rate model

$$\tilde{\chi} = c_\chi \frac{\tilde{\varepsilon}}{\tilde{k}} \widetilde{Z''^2} \tag{13}$$

with $c_\chi = 2.0$ [24] to obtain the conditional averaged scalar dissipation rate $\langle \chi_{st} \rangle$. Additionally, introducing equation 10 leads to

$$\langle \chi_{st} \rangle = \frac{c_\chi \tilde{\varepsilon}/\tilde{k} \widetilde{Z''^2}}{\int_0^1 (Z/Z_{st})^2 (\ln Z/\ln Z_{st}) \tilde{P}(Z) dZ} \tag{14}$$

This value can be computed for each cell and will be averaged over the considered spatial domain. The domain-averaged value for the conditional scalar dissipation rate at stoichiometric mixture $\langle \widehat{\chi_{st}} \rangle$ weighted with the surface of stoichiometric mixture per unit volume can be calculated as [22]

$$\langle \widehat{\chi_{st}} \rangle = \frac{\int_V \langle \chi_{st} \rangle^{3/2} \bar{\rho} \tilde{P} (Z_{st}) dV'}{\int_V \langle \chi_{st} \rangle^{1/2} \bar{\rho} \tilde{P} (Z_{st}) dV'} \tag{15}$$

Numerical Implementation

For the solution of the flow field, the FLUENT code, extended by the solution of transport equations for the mean and the variance of the mixture fraction and the mean of the enthalpy, which is defined such that it includes the heat of formation, has been applied. Turbulence is modeled by using a standard $\tilde{k} - \tilde{\varepsilon}$ model, which includes buoyancy effects and a round jet correction as proposed by Pope [25]. The calculations have been performed for a domain of 800 × 400 mm axial × radial length with 191 × 77 computational cells.

The unsteady flamelets were computed interactively with the CFD solution. The flamelet equations are solved with the mixture fraction dependence of the scalar dissipation rate from equation 10. The scalar dissipation rate at stoichiometric mixture is modeled by the domain-averaged value for the conditioned scalar dissipation rate given by equation 15. Since Meier et al. [13] found differential diffusion effects only very close to the nozzle, the calculations have been performed with unity Lewis numbers for all chemical components.

It has been shown in a previous section that close to the nozzle transient effects are negligible. The initial conditions for the unsteady flamelet have therefore been taken from a steady solution of a burning flamelet using the scalar dissipation rate at $x/D = 0$. Because all boundary conditions for the solution of the unsteady flamelet are known from the experimental conditions, only the temporal development of the scalar dissipation rate has to be known from the CFD solution. The flamelet time is calculated with equation 2, and, because only one flamelet is used to describe the whole computational domain, this flamelet time is assumed to be valid for all positions in radial direction.

The solution is obtained iteratively. At first, the mean density needed in the FLUENT calculation is obtained using a steady flamelet library. Then, the unsteady laminar flamelet is solved on a 100-point moving grid in mixture fraction space using the FlameMaster code [26]. Convergence is achieved, when the change in the scalar dissipation rate used for the flamelet calculation is lower than a prescribed tolerance.

The applied chemical mechanism consists of 40 reversible reactions among 16 chemical components including the formation of NO_x. The H_2/O_2 part has been taken from Warnatz et al. [27] and the NO_x-formation reactions are described by the thermal and the nitrous path as given by Hewson and Bollig [28].

It has been shown that transient effects hardly influence the predictions of the flow field. Therefore, the flow field can also be predicted with a steady flamelet library without radiation. From the solution of the flow field, the conditional scalar dissipation rate can be determined as a function of the flamelet time. The spatial distribution of the turbulent mean values of species mass fractions, and in particular the NO mass fractions, can then be calculated in a post-processing mode from the solution of an unsteady flamelet.

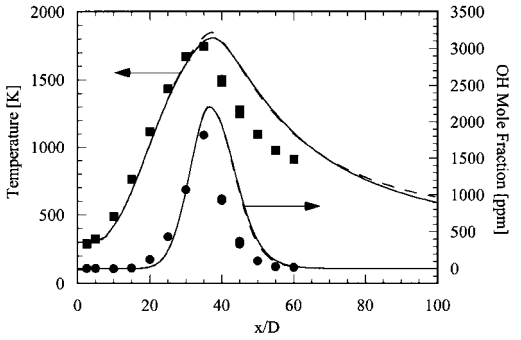

FIG. 3. Numerical results of Favre-averaged mean values of temperature and OH mole fraction along the centerline obtained by using interactive flamelet approach (*solid lines*) and steady flamelet library (*dashed lines*) compared with experimental data [14] (*symbols*).

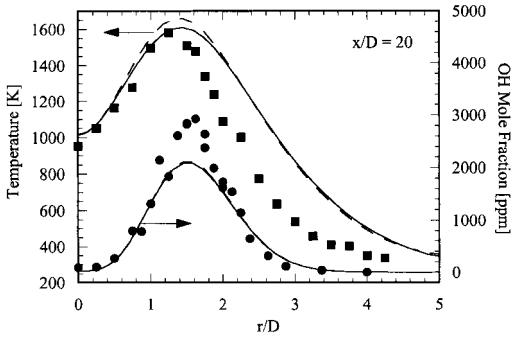

FIG. 4. Numerical results of radial profiles for Favre-averaged mean values of temperature and OH mole fraction at $x/D = 20$. See Fig. 3 for further explanation.

Results and Discussion

For the validation of the present model, a hydrogen-air diffusion flame has been used. In this configuration, which has been investigated by several groups [11–14], a volumetric mixture of 50% hydrogen, diluted with nitrogen, is injected through a nozzle with a diameter of 8 mm and a maximum centerline velocity of 42.3 m/s. The radial fuel velocity distribution is assumed to follow the 1/7-power law, which leads to a mean fuel velocity of 34.8 m/s and a Reynolds number of Re = 10,000. Coflowing air is injected through a nozzle with a diameter of 140 mm and a velocity of 0.2 m/s.

Predictions of the flow field of the investigated flame have been performed and discussed by Pfuderer [14] comparing a standard $\tilde{k} - \tilde{\varepsilon}$ model to a Reynolds stress model (RSM). It is shown that the flow field is sufficiently well described by both models, although close to the nozzle, the RSM model performs better. The flow-field predictions of the present study are similar to the $\tilde{k} - \tilde{\varepsilon}$ results shown in Ref. [14], and the presentation is therefore omitted. However, the spreading rate of the jet is slightly underpredicted and the flame length therefore too high.

In the following, the results of the numerical simulations are compared with the experimental data of Favre-averaged values of temperature, mass fractions of H_2, O_2, and H_2O, and mole fractions of OH and NO from Ref. [14]. Calculations have been performed for three different numerical models. The first is the use of steady flamelet libraries without considering radiation, for the second approach, the results of the first are used for predictions of the scalar dissipation rate and the spatial distribution of the mean mixture fraction and its variance. The Favre mean mass fractions are then computed as postprocessing from the solution of an unsteady flamelet. For the third approach, an unsteady flamelet is solved interactively with the CFD code. For the steady and the unsteady approach, apart from the unsteady term, the same flamelet equations are solved.

The temperature along the axis calculated with the interactive flamelet (solid line) and a steady flamelet library (dashed line) is compared with experimental data in Fig. 3. Corresponding radial profiles at $x/D = 20$ are given in Fig. 4. The agreement is good; although, because of the underpredicted spreading rate, the point of maximum temperature is shifted downstream. Also in the radial profile, the temperature in the lean part is too high. However, in Ref. [14], it is shown that this can be improved by the use of RSM. The results obtained by the steady flamelet library slightly overpredict the maximum temperature, compared with the interactive flamelet approach and the experimental data. At $x/D \approx 100$, the temperature from the steady library is about 90 K higher because radiation is neglected in the calculation of the steady flamelets.

In Figs. 3 and 4, also OH mole fractions are given. The agreement with experimental data is very good. The comparison of the results from the interactive flamelet and the steady flamelet library indicate that transient effects and also radiation are not important for predictions of OH concentrations in the investigated flame.

The axial mass fraction profiles of H_2, O_2, and H_2O are shown in Fig. 5. Again, the experimental data are well represented by the numerical simulation. The radial profiles, whose illustration is omitted here, show the same tendencies. The agreement with the experimental data is quite good. Corresponding to the temperature, in the lean part of the flame, the oxygen mass fraction is too low and the water mass fraction too high.

The data in Figs. 3 to 5 show that steady flamelet libraries can be used for the present case, if only the flame structure is to be described. However, this

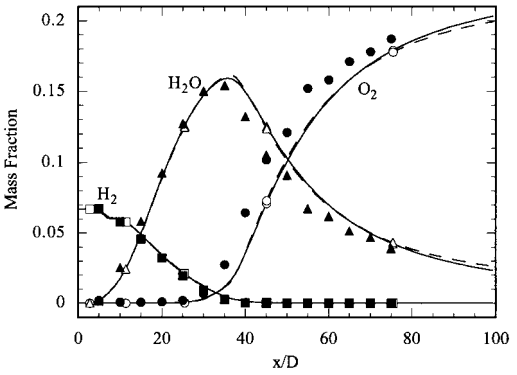

FIG. 5. Numerical results of Favre-averaged mean values of H_2, O_2, and H_2O mass fractions along the centerline. See Fig. 3 for further explanation.

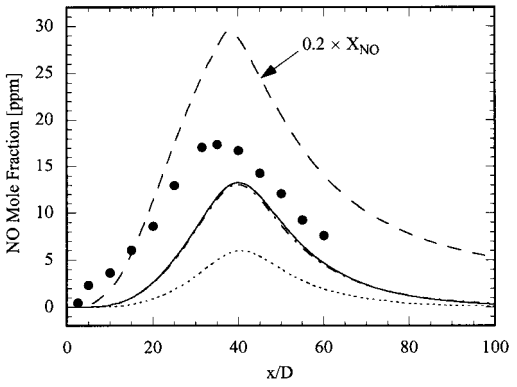

FIG. 6. Numerical results of Favre-averaged mean values of NO mole fractions along the centerline obtained by using interactive flamelet approach (*solid line*), steady flamelet library (*dashed line*), postprocessed unsteady flamelet (*dash-dotted line*), and interactive flamelet with only thermal NO (*dotted line*) compared with experimental data [14] (*symbols*).

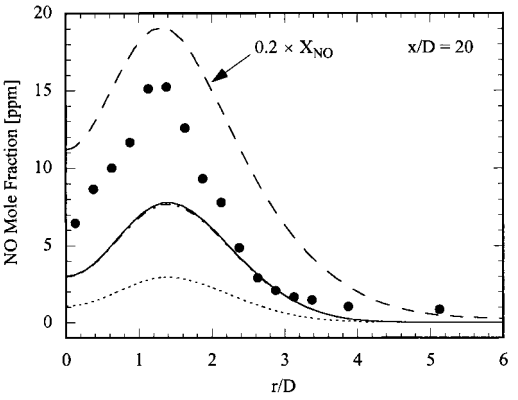

FIG. 7. Numerical results of radial profiles for Favre-averaged mean values of NO mole fraction at $x/D = 20$. See Fig. 6 for further explanation.

conclusion is not valid if slow processes are concerned. The formation of NO is known to be slow. Therefore, the steady flamelet library approach fails in predicting NO concentrations. This is shown in Figs. 6 and 7, where NO mole fractions computed with the interactive flamelet approach (solid line) and with a steady flamelet library (dashed line) are compared with experimental data. The results from the library overpredict the maximum measured NO mole fraction almost by an order of magnitude, which reveals the unsteady nature of NO formation in the considered diffusion flame. The NO profile from the interactive flamelet and the postprocessing approach underpredict the measurements by 25% and again are shifted downstream. The radial profile at $x/D = 20$ underpredicts NO even by approximately 50%. However, the overall agreement is satisfactory. Further downstream, when the position of the maximum NO concentration moves to the symmetry axis, the agreement becomes better, which can be seen from the axial comparison in Fig. 6.

The analysis of the NO-formation paths shows that a considerable contribution comes from the nitrous NO path, which is in the investigated flame favored because of the relatively low temperatures caused by nitrogen dilution of the fuel. The results of an additional calculation using the postprocessing approach where only thermal NO is considered are also depicted in Figs. 6 and 7, revealing an NO maximum, which is approximately 50% lower than for the full NO chemistry.

Conclusions

An unsteady flamelet approach is presented and validated with experimental data from a turbulent jet diffusion flame (H3-flame).

Also, it has been shown that radiation is not important for the general flame structure. Transient effects can be neglected for predictions of heat release, concentrations of major chemical components, and even the OH concentrations. Numerical simulations using steady flamelet libraries yield, therefore, good results for these quantities. However, for slow formation processes, such as the formation of NO, these have to be considered.

The interactive flamelet model is able to predict NO concentrations in reasonable agreement with experimental data. Because the unsteady flamelet depends only on the history of the scalar dissipation rate, NO can also be calculated by postprocessing.

The formation of NO by the nitrous path has been shown to contribute to approximately 50% to the

total NO production and cannot be neglected in the present case.

REFERENCES

1. Turns, S. R., *Prog. Energy Combust. Sci.* 21:361–386 (1995).
2. Chen, J. Y. and Kollmann, W., *Combust. Flame* 88:397–412 (1992).
3. Chen, J. Y., Chang, W. C., and Koszykowski, M., *Combust. Sci. Technol.* 110:505–530 (1996).
4. Peters, N., *Prog. Energy Combust. Sci.* 10:319–340 (1984).
5. Peters, N., in *Twenty-First Symposium (International) on Combustion,* The Combustion Institute, Pittsburgh, 1986, p. 1231–1250.
6. Pitsch, H. and Peters, N., "A Consistent Flamelet Formulation for Non-Premixed Combustion Considering Differential Diffusion Effects," *Combust. Flame* 114:26–40 (1998).
7. Rogg, B., Behrend, F., and Warnatz, J., in *Twenty-First Symposium (International) on Combustion,* The Combustion Institute, Pittsburgh, 1986, pp. 1533–1541.
8. Haworth, D. C., Drake, M. C., Pope, S. B., and Blint, R. J., in *Twenty-Second Symposium (International) on Combustion,* The Combustion Institute, Pittsburgh, 1988, pp. 589–597.
9. Sanders, J. P. H., Chen, J.-Y., and Gökalp, I., *Combust. Flame* 111:1–15 (1997).
10. Moss, J. B., in *Soot Formation in Combustion,* (H. Bockhorn, ed.), Springer Verlag, 1994.
11. Cheng, T.-C., Fruechtel, G., Neuber, A., Lipp, F., Hassel, E., and Janicka, J., *Forsch. Ing.—Eng. Res.* 61:165–180 (1995).
12. Pfuderer, D. G., Neuber, A. A., Früchtel, G., Hassel, E. P., and Janicka, J., *Combust. Flame* 106:301–317 (1996).
13. Meier, W., Prucker, S., Cao, M.-H., and Stricker, W., *Combust. Sci. Technol.* 118:293–312 (1996).
14. http://www.th-darmstadt.de/fb/mb/ekt/flamebase, 1997.
15. Saitoh, T. and Otsuka, Y., *Combust. Sci. Technol.* 12:135–146 (1976).
16. Barlow, R. S. and Chen, J.-C., in *Twenty-Fourth Symposium (International) on Combustion,* The Combustion Institute, Pittsburgh, 1992, pp. 231–237.
17. Mauß, F., Keller, D., and Peters, N., in *Twenty-Third Symposium (International) on Combustion,* The Combustion Institute, Pittsburgh, 1990, pp. 693–698.
18. Ferreira, J. C., Ph.D. thesis, ETH Zürich, 1996.
19. Hubbard, G. L. and Tien, C. L., *J. Heat Transfer* 100:235–242 (1978).
20. Kim, J. S. and Williams, F. A., *SIAM J. Appl. Math.* 53:1551–1566 (1993).
21. Bish, E. S. and Dahm, W. J. A., *Combust. Flame* 100:457–464 (1995).
22. Pitsch, H., Ph.D. thesis, RWTH Aachen, 1998.
23. Hellström, T., private communication, 1997.
24. Jones, W. P. and Whitelaw, J. H., *Combust. Flame* 48:1–26 (1982).
25. Pope, S. B., *AIAA J.* 16:279–281 (1978).
26. Pitsch, H. and Bollig, M., *FlameMaster, A Computer Code for Homogeneous Combustion and One-Dimensional Laminar Flame Calculations,* Institut für Technische Mechanik, RWTH Aachen.
27. Warnatz, J., Maas, U., and Dibble, R. W., *Combustion, Physical and Chemical Fundamentals, Modeling and Simulation, Experiments, Pollutant Formation,* Springer-Verlag, New York, 1996.
28. Hewson, J. C. and Bollig, M., in *Twenty-Sixth Symposium (International) on Combustion,* The Combustion Institute, Pittsburgh, 1996, pp. 2171–2179.

COMMENTS

Nigel S. A. Smith, Aeronautical and Maritime Research Laboratory, Australia. Please indicate if differential diffusion of species was included in the laminar flame computations employed in the model described.

If differential molecular transport was employed, then surely the results of such modeling would predict conditional mean reactive species profiles in the downstream region of jet flames with features such as superequilibrium temperature levels on the lean side of stoichiometric. Such conditionally averaged profile details have not been observed experimentally by Barlow and coworkers.

If, on the other hand, uniform diffusivities were employed in the laminar flame computations, what possible justification could be offered for this assumption in the context of a laminar diffusion flame? Surely if local flame structure in turbulent flames is assumed to correspond to actual laminar flamelets, then differential diffusion must be included in determining the structure of the flamelets.

Surely the absence of differential diffusion effects in measured conditional mean data in the open literature, far downstream in jet flames, is an indicator of the local inapplicability of the one-dimensional laminar diffusive transport assumption that forms the basis of flamelet modeling.

Author's Reply. Differential diffusion was not included in the flamelet calculations, which have been performed with the assumption that all Lewis numbers are unity. The experimental data for the investigated flame obtained by Meier et al. ([13] in the paper) indicated that there are strong differential diffusion effects close to the nozzle, which vanish at approximately $\chi/D = 20$. The physical explanation in terms of the flamelet model is that close to the nozzle, the scalar dissipation rate is high, which indicates a very thin mixing layer. If the mixing layer is thinner than

the smallest turbulent eddies, mixing is controlled by molecular diffusion. Farther downstream, when the scalar dissipation rate decreases, the mixing layer broadens and becomes thicker than the small scales of the turbulence, which then contribute to the mixing within this layer and the effective Lewis numbers become unity. Because in the investigated configuration the reaction zone is still much thinner than the small scales of the turbulence, the flamelet assumption is still applicable. The incorporation of the differential diffusion effects close to the nozzle in the presented model will be done in the future.

•

Godfrey Mungel, Stanford University, USA. You attribute the poorer agreement farther downstream to the assumption $Z = 1$. However, past the potential core of the jet, by definition, $Z < 1$ and continues to decrease with downstream distance. Why did you not include this effect in your calculation, and why is your claim correct?

Author's Reply. I mentioned that the overprediction of the calculated temperature might be caused by the assumption that Z_{max} in equation 10 is equal to unity. This affects the distribution of the scalar dissipation rate significantly, when the $Z_{max} < Z_{st}$. A flamelet formulation for the inclusion of varying Z-space boundaries is given (Ref. [22] in the paper). This model will be applied to steady jet flames in the future. However, further investigations have shown that the calculated profiles agree much better with the experimental data, when these are plotted over the mean mixture fraction. This indicates that the disagreement mainly arises from errors in the predictions of the mixture fraction.

•

Assaad R. Masri, The University of Sydney, Australia. Would you please comment on the relative importance of accounting for radiation and unsteady effects on the rates of formation of NO with increasing axial distance.

Author's Reply. Figure 6 shows that the NO mole fraction is overpredicted by an order of magnitude, if unsteady effects are neglected. This is not influenced by the axial nozzle distance. Figure 1 shows that, if unsteady effects are neglected, the errors for also neglecting radiative effects are much smaller than considering radiation. However, both assumptions are getting worse with increasing axial nozzle distance. Figure 3 and 4 show that the steady approach neglecting radiation overpredicts the temperature by approximately 50–100 K, which is known to have a large influence on the formation rates of NO.

•

George Kosàly, University of Washington, USA. In our experience, the detailed modeling of the scalar dissipation rate is of secondary importance in hydrogen/air. Correct prediction can be obtained, that is, by using the average value at the radial position where the mixture fraction hits its stoichiometric value.

Author's Reply. This is true for very small values of the scalar dissipation rate, if the Lewis numbers of all chemical species are assumed to be unity. However, if the effects of nonequal Lewis numbers are considered, large differences remain, even for very low values of the scalar dissipation rate. In the present study, differential diffusion effects have been neglected, but the scalar dissipation is too high to justify the assumption of a constant scalar dissipation rate.